ELSEVIER

Catalysis Today 54 (1999) 495–505

CATALYSIS TODAY

www.elsevier.com/locate/cattod

The bifunctional reaction pathway and dual kinetic regimes in NO_x SCR by methane over cobalt mordenite catalysts

J.R. Regalbuto [a,*], T. Zheng [a], J.T. Miller [b]

[a] *University of Illinois at Chicago, Department of Chemical Engineering, 810 S. Clinton St., Chicago, IL 60607, USA*
[b] *Amoco Research Center, E-1F, 150 W. Warrenville Rd., Naperville, IL 60563, USA*

Abstract

The pathway for selective reduction of NO_x by methane over Co mordenite catayst has been studied by comparing the rates of the individual reactions (NO oxidation, CH_4 oxidation, NO_2 reduction) with that of the combined reaction ($NO + O_2 + CH_4$). $Co^{(+2)}$ was exchanged into H-MOR and Na-MOR to give catalysts with different metal loading and number of support protons. Additionally, exchanged $Co^{(+2)}$ ions were precipitated with NaOH to produce dispersed cobalt oxide on Na-MOR. The NO oxidation rate is the same for ion exchanged $Co^{(+2)}$ ions in H-MOR and Na-MOR, but the rate of $Co^{(+2)}$ ions is much lower than that of cobalt oxide. NO oxidation equilibrium is obtained only for those catalysts with high metal loading, cobalt oxide or run at low GHSV. Under the conditions of selective catalytic reduction, methane oxidation by O_2 is low for all catalysts. The turnover frequency of Co on Na-MOR, however, is higher than that on H-MOR. The rate of NO_2 reduction to N_2 is directly proportional to the number of support acid sites and independent of the amount of Co. Comparison of the rates and selectivities for the individual reactions with the combined reaction of $NO + O_2 + CH_4$ indicates that there are two types of catalysts. For the first, the NO oxidation is in equilibrium and the rate determining step is reduction of NO_2. For these catalysts, the rate (and selectivity) for formation of N_2 is identical from $NO + O_2 + CH_4$ and $NO_2 + CH_4$. These catalysts have high metal loading and few acid sites. Nevertheless, the rate of N_2 formation increases with increasing number of protons. For the second type of catalyst, NO oxidation is not in equilibrium and is the rate limiting step. For these catalysts the rate of N_2 formation increases with increasing metal loading. Neither catalyst type, however, is optimized for the maximum formation of N_2. By using a mixture of catalysts, one with high NO oxidation activity and one with a large number of Brønsted acid sites, the rate of N_2 is greater than the weighted sum of the individual catalysts. The current results support the proposal that the pathway for selective catalytic reduction is bifunctional where metal sites affect NO oxidation, while support protons catalyze the formation of N_2.

Keywords: Selective catalytic reduction; Lean NO_x reduction; Co-mordenite; NO_2 reduction; NO oxidation; Methane oxidation

1. Introduction

Oxides of nitrogen which are by-products of high temperature combustion, contribute to acid rain and promote the formation of ozone and smog. Current and future environmental legislation is likely to put ever increasing demands on the reduction of these harmful pollutants. While selective catalytic reduction of NO by ammonia is the most widespread method for flue gas clean up from stationary sources, reduction of NO_x from mobile sources requires catalysts which utilize exhaust hydrocarbons as the reducing agent. While the current auto emission catalysts are based on noble metals, there has been a great deal of research on development of metal exchanged zeolite catalysts such as Cu and Co ion exchanged into ZSM-5, which

* Corresponding author.

0920-5861/99/$ – see front matter
PII: S0920-5861(99)00212-6

permit engine operation in the fuel efficient, lean burn regime.

For the latter catalysts, there has evolved general agreement that the first step in the selective catalytic reduction pathway is the oxidation of NO to NO_2, and the second step, NO_2 to N_2 proceeds through a series of poorly understood reactions. There is also agreement that strong zeolite acidity is needed for high activity using methane as a reductant. There is no consensus, however, over which type of catalytic site each of the two steps occurs.

There are three main avenues of thought on the types of catalytic sites in metal exchanged zeolites for lean NO_x reduction. The first is that the mechanism is in part a free radical reaction, to some extent independent of a catalytic surface, in which methyl radicals are generated by NO_2 [1,2]. The active catalytic sites have not been specified in these studies. The second school is that both the NO oxidation and NO_2 reduction steps occur over the metal (ion) sites [3–6]. The role of the acidic support is thought to be indirect, for example in promoting the reactions via crystal field effects in $Co^{(+2)}$/ZSM-5 [5] or by stabilizing Pd(+2) in this ionic state in Pd/ZSM-5 catalysts [6]. A number of earlier works established that proton sites in strongly acidic zeolites have appreciable activity for NO oxidation and NO_2 reduction [7–9], and a landmark work with physical mixtures of Pd/SiO_2 and strongly acidic (even non-zeolitic) materials [10] strongly suggested the bifunctional nature of the reaction mechanism.

In the third vein, a growing number of groups now cite a bifunctional NO_x reduction mechanism involving both metal and acid cites [11–16]. Here again, confusion exists over which site is responsible for which function. Both types of sites in Cu/H-ZSM-5 have been suggested to act in parallel for both reactions [11]. In another series of works on Ga/H-ZSM-5 and In/H-ZSM-5, NO oxidation is attributed to the proton sites and NO_2 reduction to the metal sites [12,13]. On the other hand, NO oxidation is reported to be enhanced by physically mixing Ce and Mn oxides with Ce-ZSM-5 ([14] and references within). In studies of Pd/H-ZSM-5 catalysts reviewed in the same paper [14], Pd sites are thought responsible for activating methane and assisting proton sites in NO oxidation, and NO_2 reduction is claimed to occur entirely over the proton sites.

To sort through all these possibilities, our approach has been to isolate the reaction steps, and to isolate the metal and proton catalyst functions. In an earlier work, the overall ($NO + O_2 + CH_4$) reaction was broken down into the individual reactions of ($NO + O_2$) and ($NO_2 + CH_4$) [15]. At the same time, the catalyst functions were isolated by preparing metal free catalysts with only proton sites and proton free catalysts with only metal (ion and oxide) sites, in addition to catalysts that contain both types of sites. We proposed that the selective catalytic reduction pathway was bifunctional with NO oxidation catalyzed by metal sites, and NO_2 reduction catalyzed by support proton sites. The strategy of isolating catalytic functions was also utilized in a recent study of physical mixtures of Co/Al_2O_3 and protonated zeolites [16]. These authors reached the same conclusion, namely, that the metal function was that of NO oxidation, and the proton site catalyzed NO_2 reduction.

In the present study, we compare the rates and selectivities of the individual reactions ($NO + O_2$), ($NO_2 + CH_4$), and ($CH_4 + O_2$) with the overall ($NO + O_2 + CH_4$) reaction for a number of Co-mordenite catalysts containing different metal loadings and number of support protons. These results support the proposal that the selective catalytic reduction of NO_x is bifunctional and that the metal ion or oxide is the active site for NO oxidation, while zeolite acid sites catalyze the reduction of NO_2. In addition, depending on the catalyst composition and reaction conditions, either reaction may be rate determining. The existence of two kinetic regimes at commonly employed experimental conditions reconciles many contradictory results in the literature. An improved process for NO_x reduction is suggested whereby the two separate catalyst functions are optimized independently.

2. Experimental

2.1. Catalysts

Na-mordenite (CBV-10A, 5.6 wt% Al) was a commercial zeolite obtained from PQ (now Zeolyst). 100 g of Na-MOR (NaMOR) was ammonium exchanged with 3×500 ml of 2 M NH_4NO_3 and calcined at 450°C to give H-MOR (HMOR). Cobalt catalysts were prepared by conventional ion exchange with

Table 1
Catalyst compositions

Catalyst (designation)	Al (wt%)	Co (wt%)	Exchange (%)	Na (wt%)	H^+ Content (mmol/g)
H-MOR (HMOR)	5.8	–	0	–	1.74
1% Co/H-MOR (1 Co/H)	5.6	0.74	12	–	1.50
1% Co/Na-MOR (1 Co/Na)	5.4	0.95	16	4.18	0.05
3% Co/H-MOR (3 Co/H)	5.7	3.15	51	–	1.53
4% Co/Na-MOR (4 Co/Na)	5.5	3.80	62	2.09	0.68
4% CoO_x/Na-MOR (CoO_x)	5.5	4.06	–	3.19	0.39

cobalt nitrate. Cobalt was chosen since it is one of the most active exchanged metals reported for this reaction. In order to obtain 1 wt% Co, the zeolite was exchanged with a limited amount of cobalt nitrate. For example, 1.5 g $Co(NO_3)_2$ $6H_2O$ dissolved in 200 ml H_2O was added to 25 g of H-mordenite (H-MOR) (ca. 1.2 wt% Co based on the amount of support). The zeolite was heated to 60°C for 3 h and filtered. The Co/H-MOR was re-slurried in 200 ml of hot H_2O for 2 h, filtered, dried overnight at 100°C and calcined by heating at 1 C/min in flowing air to 450°C and holding for 1 h. The color of the $Co^{(+2)}$ exchanged zeolites was pink. Co exchange of Na-MOR also resulted in the partial exchange of Na^+ by H^+ ions. Cobalt oxide within the pores of Na-MOR (25 g) was prepared by 3×200 ml cobalt exchange with 0.5 M $Co(NO_3)_2$ $6H_2O$ at 60°C. Following the final exchange, the excess Co solution was removed by water washing. To a slurry of Co/Na-MOR, NaOH was added slowly keeping the pH about 9. After ca. 15 min the pH decreased to ca. 5 and more NaOH was added until the pH remained 9. The catalyst was filtered, washed, dried and calcined as before. The calcined CoO_x/Na-MOR catalyst was black in color. Elemental analysis for Co, Al and Na were obtained by inductive coupled plasma. The number of acid sites was determined by temperature programmed desorption of NH_3, using a maximum desorption temperature of 600°C and deconvoluting the high temperature (400°C) peak corresponding to Brønsted sites from the lower temperature Lewis site peak. The proton contents in mmol H^+/g catalyst 1.74 are included in Table 1.

2.2. Catalytic reactions

Catalytic activities and selectivities were determined in a 1.25 cm i.d., quartz, plug-flow micro-reactor at atmospheric pressure. The thermocouple was in contact with the catalyst bed, and the reaction temperature was 400°C. The gas flow rates were controlled by Brooks 5872 mass flow controllers, and the reactant composition was obtained by mixing five different gasses (NO/He, NO_2/He, O_2/He, CH_4/He and He). For each catalyst, four separate reactions were studied: NO_2 decomposition, NO_2 reduction to N_2 with CH_4, CH_4 oxidation by O_2 and $NO + O_2 + CH_4$ to N_2. Activity for the NO-CH_4 reaction was also measured and found to be insignificant over all catalysts. The composition of the reaction mixtures were 1200 ppm NO or NO_2, 2.5 wt% O_2, and 1000 ppm CH_4 (balance He). The outlet composition was analyzed by on-line gas chromatography equipped with a TCD detector (5890 HP with an 1/8 in. × 8 ft. 5 Å molecular-sieve column for O_2, N_2, CO and CH_4 plus a 1/8 in. × 6 ft. Porapack R column for CO_2 and C_3H_6) and a Rosemont Analytical Model 591 A chemiluminesence analyzer. Approximately 0.1–0.4 g of catalyst was crushed and screened to 20/40 mesh and the gas hourly space velocity was varied between 2000 and 27 000 h^{-1} in order to keep the conversion between 10 and 30% for each reaction. The selectivity for NO_x reduction $[N_2/(CO_2 + CO)]$ was determined at a 20% yield of N_2 by adjusting the space velocity. In order to minimize background NO oxidation/NO_2 decomposition in the lines leading to the micro-reactor, plastic tubing was used.

3. Results and discussion

To examine the extent to which NO oxidation/NO_2 decomposition approaches equilibrium in the overall reaction, NO_2 decomposition rates were measured directly. Absolute rates for the decomposition of NO_2 at 400°C for the series of mordenite supported catalysts

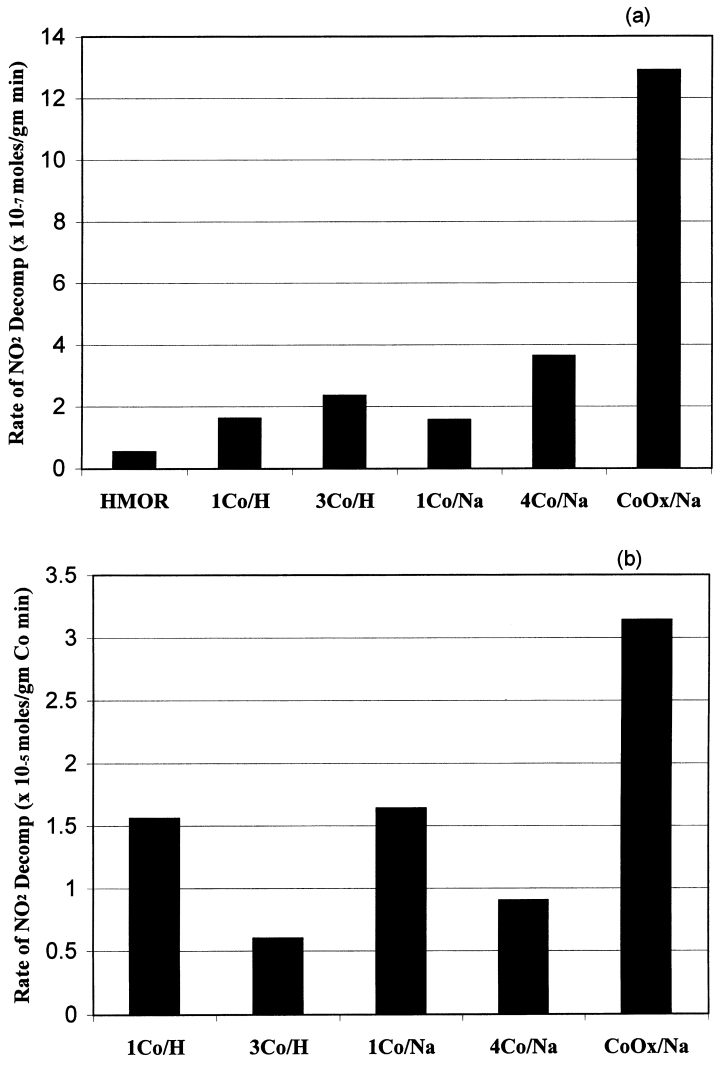

Fig. 1. The rate of NO_2 decomposition at 400°C, 1200 ppm NO_2 and 2.5% O_2, (a) absolute rate and (b) specific rate (per gm Co).

are shown in Fig. 1(a). The rates normalized by the Co weight loading and corrected for the activity due to the number of acid sites are shown in Fig. 1(b). First, the catalyst containing CoO_x is much more active than the other ion exchanged $Co^{(+2)}$ catalysts. It was noted previously that the rate per $Co^{(+2)}$ was independent of the support for NO oxidation at 300°C [15]. Similarly, the two low loading catalysts (1% Co/HMOR, 1% Co/NaMOR) have the same rate per Co, even though one support is strongly acidic while the other has few acid sites.

In Fig. 1(b), however, the per Co rate for the highest two loadings, 3.15 and 3.8 wt% Co, are somewhat less than that of the low loaded catalysts. Given the relatively high rates for the latter two and the high Co concentrations, these differences might be due to diffusion limitations. The minimum value of the Weisz–Prater criterion for the two high Co catalyts can be estimated by assuming a conservatively high effective diffusivity of 10^{-3} cm^2/s [17]. This yields a value of 1.2 for the 1% Co/HMOR and 1% Co/NaMOR, and 1.8 and 2.7 for the 3% Co/HMOR and 4% Co/NaMOR, re-

spectively. Since these values are greater than unity, diffusion limitations are expected for all catalysts but might not be manifested in the lowest loading catalysts if the metal resides near the exterior of the zeolite particles.

Calculations based on the rates and the (single) turnover frequency for NO oxidation derived from this data will be presented later. As noted earlier [15], the assumption that this reaction is rapid and in equilibrium is often incorrect.

If the principle function of the metal is to oxidize NO to NO_2, the metal function may be circumvented by reduction with NO_2 as the feed. In this way, the inherent rate of a catalyst to convert NO_2 to N_2 with methane can be directly measured. In Fig. 2, the rate of N_2 formation and the selectively of all catalysts are given for the reaction between NO_2 and CH_4 at 400°C. The most active and selective catalyst is the metal free, strongly acidic H-MOR. The $Co^{(+2)}$ exchanged H-MOR catalysts are slightly less active and selective, while the $Co^{(+2)}$ Na-MOR catalysts are poorly active and selective. The effect of acid strength has previously been noted [15] for USY and SiO_2–Al_2O_3 catalysts which possess higher densities of proton sites than H-MOR, yet are much less active suggesting that the proton sites of the zeolites, and especially the strongly acidic protons, are responsible for the conversion of NO_2 to N_2.

The ability of the mordenite catalysts to oxidize methane at 400°C is illustrated in Fig. 3, first as rates per gram of catalyst in Fig. 3(a), and then as rates per Co in Fig. 3(b). Comparing Figs. 2 and 3, it is seen that the rate of methane oxidation is 10 to a 100-fold lower with oxygen than with NO_2, especially for the ion exchanged $Co^{(+2)}$ in H-MOR. Given that the oxygen concentration is 20 times that of the NO_2, the rate constant for methane oxidation by NO_2 is greater than that for oxidation by O_2 by ca. 200–2000.

In contrast to NO oxidation, the effect of the zeolite composition on methane oxidation is significant: the effect of Na^+ is to increase the activity of $Co^{(+2)}$ ions by about an order of magnitude (Fig. 3(b)). Thus, the selectivity of the Na catalysts for the NO_2-CH_4 reaction seen in Fig. 2(b) is poor not only due to a lack of proton sites leading to a low rate of N_2 formation, but also because the methane oxidation activity of the metal is relatively higher.

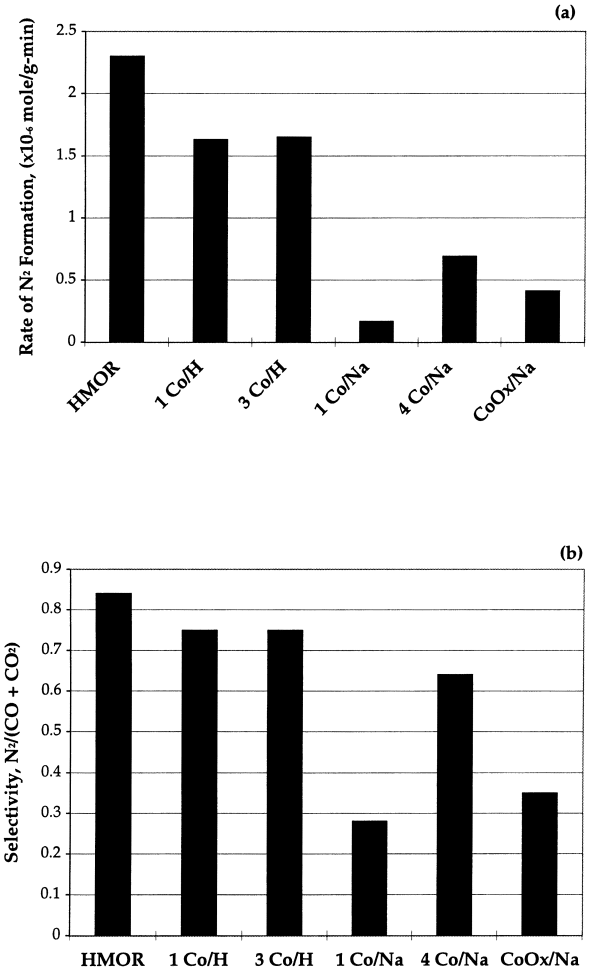

Fig. 2. Reduction of NO_2 with methane at 400°C, 1200 ppm NO_2 and 1000 ppm CH_4, (a) rate of N_2 formation, and (b) selectivity $[N_2/(CO_2 + CO)]$ at 20% N_2 conversion.

The rates and selectivity for the overall $NO + O_2 + CH_4$ reaction are shown in Fig. 4. These measurements were made at a conversion of NO to N_2 of 20%, and required different space velocities for the different catalysts. The space velocities for 20% conversion and the N_2 formation rates for all catalysts are given in Table 2. The ratio of the GHSVs (or the rates) reflects the differences in activity of the catalysts.

The effect of proton sites on the rate of N_2 formation seen in Fig. 2 for the reaction of $NO_2 + CH_4$ is not clearly manifested in the rate data for the overall reaction (Fig. 4(a)). The rates for the Na-MOR are about the same as for H-MOR. The rate of N_2 formation

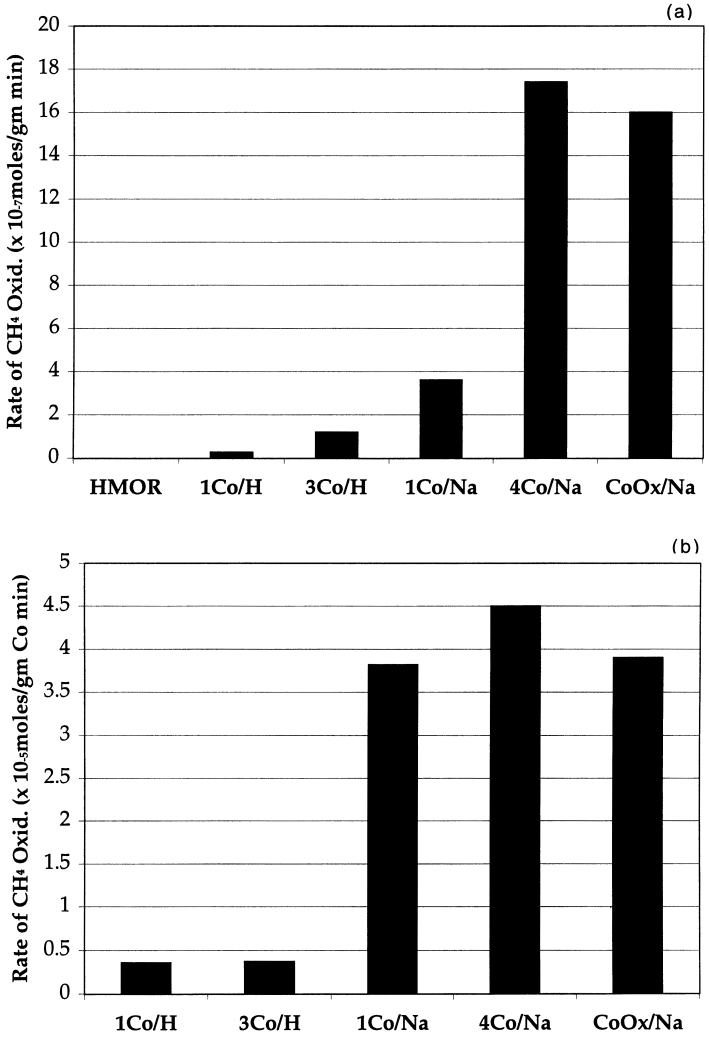

Fig. 3. Rates of CH_4 oxidation at 400°C, 1000 ppm CH_4 and 2.5% O_2, (a) absolute rates and (b) rates per gm Co.

Table 2
Overall reaction rates and space velocites for 20% conversion of NO to N_2

Catalyst	Rate of N_2 formation[a] (mol N_2/gm min)	GHSV
HMOR	2.7×10^{-7}	2250
l Co/H	4.0×10^{-7}	3300
3 Co/H	8.8×10^{-7}	7300
1 Co/Na	1.7×10^{-7}	1420
4 Co/Na	8.0×10^{-7}	6630
CoO_x	4.5×10^{-7}	3760

[a] 1200 ppm NO, 1000 ppm CH_4, 2.5 wt% O_2, 400°C.

for the metal free H-MOR is now relatively low, and the rate in general appears to increase with increasing metal loading. The selectivity (Fig. 4(b)) does appear similar to that in Fig. 2, where selectivity is lowest for those catalysts containing Na^+. Similar selectivities for the overall reaction over mordenite catalysts, in the range of 0.1–0.7 mmol H^+/gm, were reported recently by Pentuchi [18] at a temperature of 525°C.

It is useful to compare the rate of N_2 formation for the overall reaction to that from $NO_2 + CH_4$. Shown in Fig. 5(a) and (b) are the activity and selectivity for

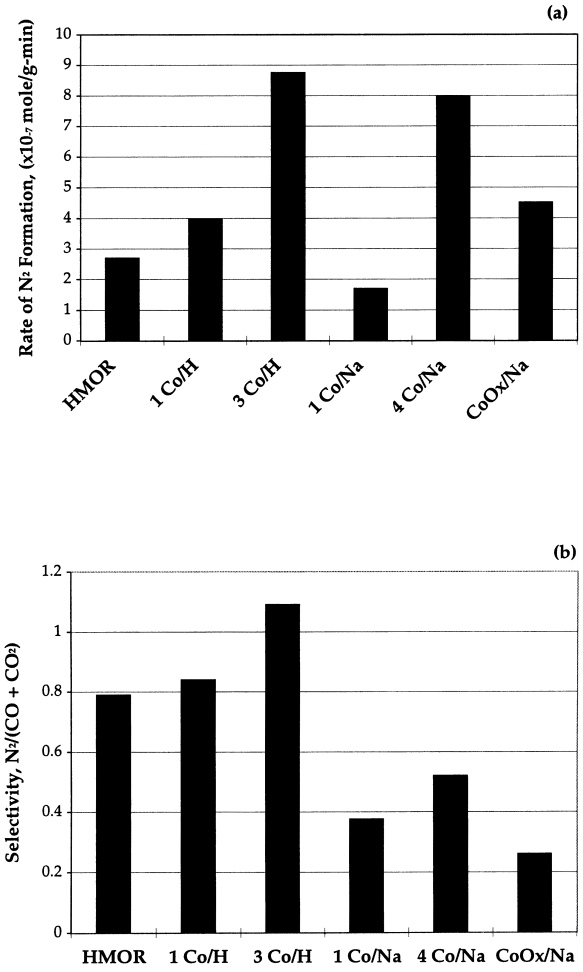

Fig. 4. Rate of N_2 production from the overall ($NO + O_2 + CH_4$) reaction at 400°C, 1200 ppm NO_2 and 1000 ppm CH_4, (a) rate of N_2 formation, and (b) selectivity [$N_2/(CO_2 + CO)$] at 20% N_2 conversion.

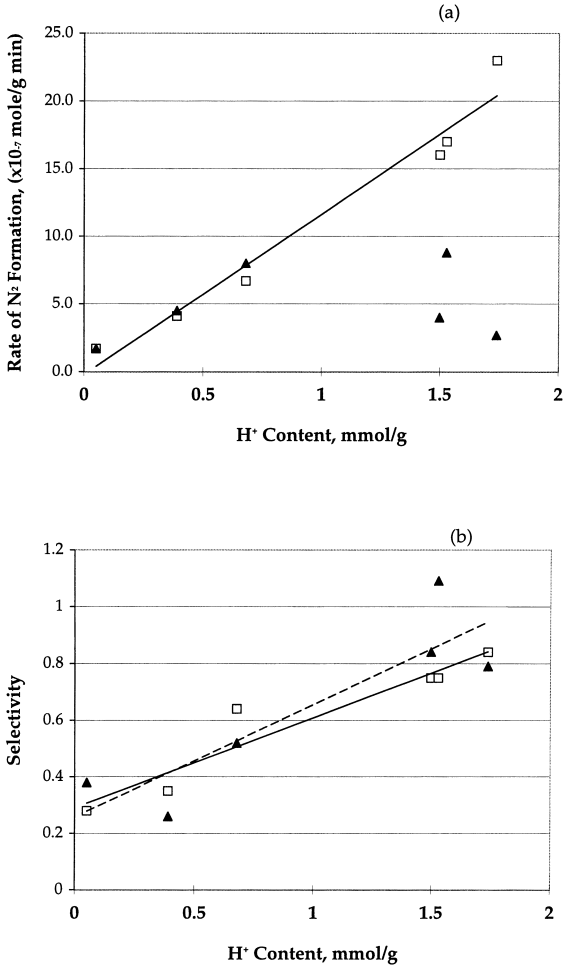

Fig. 5. Correlation of the (a) N_2 production rate and (b) selectivity for the $NO_2 + CH_4$ reaction (unfilled squares) and ($NO + O_2 + CH_4$) reaction (filled triangles).

$NO + O_2 + CH_4$ (filled triangles) and $NO_2 + CH_4$ (unfilled triangles) versus the number of protons of the support. The three pairs of points on the left side of Fig. 5(a), corresponding to the Na-MOR catalysts, reveal that the rates are the same for both reactions and are proportional to the number of acid sites. The data on the right side of Fig. 5(a), i.e., those for the H-MOR catalysts, indicate that the rates of $NO_2 + CH_4$ (unfilled squares) are higher than those for overall reaction (filled triangles). The linear correlation previously reported [15] between the rate of N_2 formation from $NO_2 + CH_4$ (all unfilled squares) with proton content of the support was the primary evidence for the role of acid sites in the reaction pathway for the catalytic reduction of NO_x by hydrocarbons. Why then does this correlation fail for the $NO + O_2 + CH_4$ reaction?

The catalysts can be grouped into two types according to which of the two reaction steps, NO oxidation or NO_2 reduction, is rate determining. On the left hand side of Fig. 5(a), the rate of NO oxidation is relatively fast and the activity is limited by the numbers of Brønsted sites for the conversion of $NO_2 + CH_4$ to N_2. Since the number of protons sites is rate limiting there is a linear increase in the rate of N_2 formation with increasing number of acid sites. Conditions which favor high rates of NO oxidation are catalysts

with high metal loadings or metal oxides, high reaction temperatures and low GHSV. On the right hand side of Fig. 5(a), the rate of NO oxidation is low and becomes rate limiting. The number of acid sites is sufficient to convert NO_2 to N_2, thus more acid sites does not lead to higher activity. Catalysts and reaction conditions where the rate of NO oxidation becomes rate limiting are catalysts with low metal loading, low reaction temperatures and high GHSV. Additionally, the catalysts must contain a significant number of strongly acidic protons. Under these conditions there will be no correlation between the rate of N_2 formation and the number of protons.

To more quantitatively evaluate the effect of the rate of NO oxidation on the rate of selective catalytic reduction of NO_x, the conversion to NO_2 for each catalysts has been calculated at the space velocity employed for the overall rate determination (Table 2). The diffusion-free rate of NO_2 decomposition in Fig. 1(b) (1.5×10^{-5} mol/gm Co min at 1200 ppm NO_2 and 2% O_2) was converted to an NO oxidation rate constant using the equilibrium constant for the $NO + O_2 = NO_2$ at 400°C, 722 l/mol [19]. This gives a rate constant of 3600 (cm^3/gm Co min), which can be considered the intrinsic rate constant for NO oxidation over $Co^{(+2)}$ ions in zeolite supports. Calculations for the conversion of NO to NO_2 at the space velocities of the overall reactions were then made by assuming a reversible first order reaction and are shown in Fig. 6. The NO conversion is lowest for the three H-MOR catalysts, due to low Co loading (HMOR and 1% Co/HMOR) or high space velocity (3% Co/HMOR). For the three NaMOR catalysts, the space velocity was either very low (1% Co/NaMOR) or the metal loading was high enough (or was CoO_x) such that NO conversion was higher and indeed approached equilibrium in two of the three cases.

When the rate of NO oxidation is rate limiting the dependence of the rate on the number of acid sites will not be observed. For example, when the rate of N_2 formation is plotted versus wt% Co as in Fig. 7 (filled triangles), a correlation appears for the H-MOR catalysts. These are the types of catalysts most often prepared in the literature for this reaction. A rougher correlation is seen for the NaMOR catalysts. While there is a correlation of the metal loading with the selective catalytic reduction reaction for the HMOR catalysts, there is no correlation for the $NO_2 + CH_4$ reaction (open squares). Under reaction conditions and with catalysts where the rate limiting step is NO oxidation, it could easily be concluded that the metal sites are the only active site for selective catalytic reduction with methane.

Using the rate constant for NO oxidation given above, the wt% Co necessary to achieve 90% conversion of equilibrium at 400°C has been plotted versus

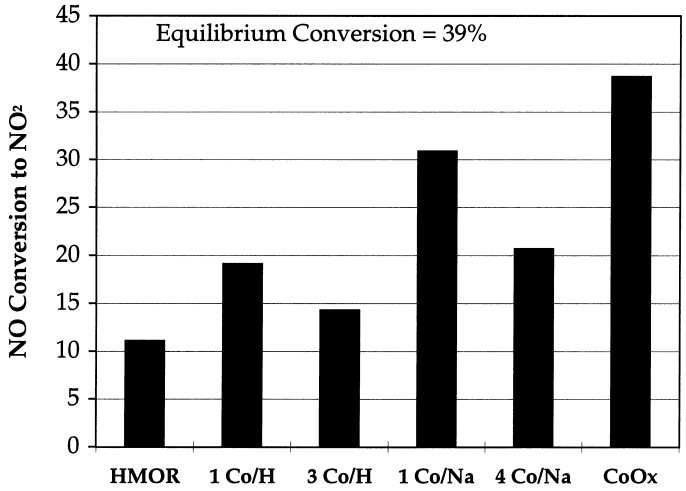

Fig. 6. Conversion estimations for NO oxidation to NO_2 at the space velocities employed in the ($NO + O_2 + CH_4$) runs (Table 2). A first order, reversible reaction is assumed.

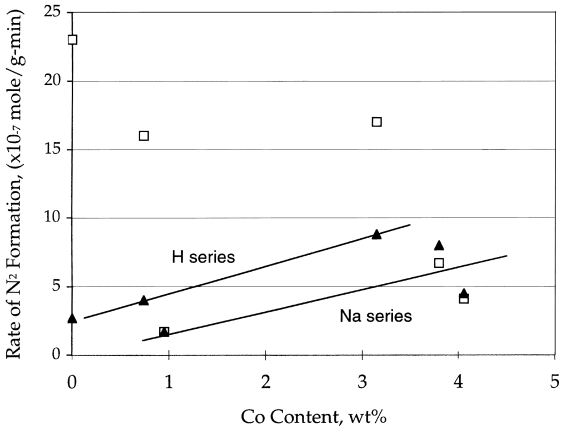

Fig. 7. Attempted correlations of the rate of N_2 formation to weight % Co for the $NO_2 + CH_4$ reaction (unfilled squares) and ($NO + O_2 + CH_4$) reaction (filled triangles).

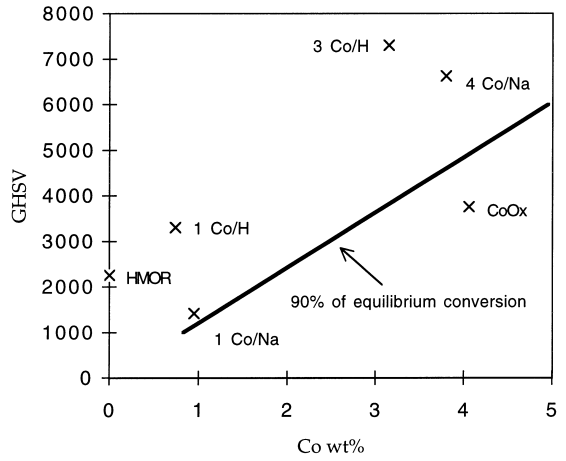

Fig. 8. Estimation of the amount of $Co^{(+2)}$ required for 90% NO conversion to NO_2 at various space velocities.

the GHSV in Fig. 8. Since the composition of the zeolite support has almost no effect on the NO oxidation activity of $Co^{(+2)}$ [15], Fig. 8 may be employed for other catalysts containing $Co^{(+2)}$ ions (no CoO_x) and where the zeolite has low NO oxidation activity. The region above and to the left (lower metal loadings, higher space velocity) represents the region where NO oxidation becomes rate limiting, while the region below and to the right of this curve (higher metal loadings, lower space velocity) represents the region free of NO oxidation limitations. The HMOR and NaMOR catalysts of the present work have been superimposed on this plot, once again showing the NO oxidation limitation of the HMOR catalysts.

It appears that rate data for the selective reduction of NO_x is often taken at conditions where NO oxidation is rate limiting. For example, Misono and coworkers recently demonstrated that there is a decrease in the CD_4–CH_4 kinetic isotope effect as temperature decreases and this was attributed to the slow NO oxidation rate at lower temperatures [20]. Over a series of Co/ferrierite catalysts with Co loadings from 1.3 to 2.7 wt%, the rate of N_2 formation for the overall reaction was very clearly proportional to the metal loading over a wide range of temperatures [21]. These catalysts were tested at space velocities from 100 000 to 200 000 h^{-1} which places the Co/FER above the curve apparently far from NO oxidation equilibrium. Without this realization, the rate dependence on Co concentration as appears in Fig. 7 would be the basis for proposing a mechanism occurs entirely over Co sites. Notably, these authors also compared the rates of $NO + O_2 + CH_4$ and $NO_2 + CH_4$ reactions. At 400°C, the rate of N_2 formation from NO_2 was twice the rate from $NO + O_2$ (Table 1 of Ref. [21]). This difference diminished with increasing reaction temperature. These results are consistent with the results reported here for the Co–HMOR catalysts, i.e., those on the right side of Fig. 5(a). The rate is faster for the NO_2 case since the NO oxidation limitation is overcome.

Another example where we believe slow NO oxidation masks the role of proton sites is a series of ZSM-5 catalysts with increasing Co loading [22]. For the overall reaction, the rate of N_2 formation increases up to a Co/Al ratio of ca. 0.34. With further increases in Co loading, however, the rate does not increase. In contrast to other zeolite supports, the Brønsted sites in ZSM-5 display high activity for NO oxidation [15,16,23,24], therefore, Fig. 8 cannot reliably be used. Nevertheless, direct measurements of rate of NO oxidation over Co/ZSM-5 suggest that equilibrium is often not obtained. For a 1.2 wt% Co/ZSM-5 catalyst, for example, NO oxidation equilibrium was attained at 400°C and above at a space velocity of 15 000 h^{-1} [16]. At 400°C and 45 000 h^{-1}, however, NO conversion was only ca. 30% to equilibrium over a 4 wt% Co/ZSM-5 [5,25].

A set of results with ZSM-5 catalysts which is contradictory to the results in Fig. 2 is one where the rate of N_2 formation from $NO_2 + CH_4$ is from two [26] to

five [5,6] times higher for Co/ZSM-5 than H-ZSM-5. (With nitromethane as a feed, however, both catalysts have the same activity for N_2 production [27]. While the number of protons in these catalysts were not measured, presumably H-ZSM-5 has more protons than do the $Co^{(+2)}$ exchanged zeolites. If ZSM-5 behaved similarly to mordenite, H-ZSM-5 would be expected to have higher activity for the $NO_2 + CH_4$ reaction. A possible explanation for this discrepancy may stem from the different CH_4/NO_2 ratio employed in those works (2800 ppm/2100 ppm = 1.25 versus 1000/1200 = 0.83), and be related to the unique ability of ZSM-5 to oxidize NO. In our previous paper, we suggested that methane activated on proton sites interacts with NO_2 in the gas phase. If over ZSM-5, NO_2 is adsorbed on the surface, the higher methane/NO_2 ratio could cause inhibition of NO_2 adsorption, which would be alleviated in the case of Co/ZSM-5. These remarks are highly speculative and the apparent difference between ZSM-5 and mordenite materials must be studied further.

The latter ZSM-5 study notwithstanding, the current data and that in the literature is consistent with the hypothesis of a bifunctional reaction pathway for lean NO_x reduction with hydrocarbons, where NO oxidation occurs primarily at metal sites (except for proton sites in ZSM-5) and NO_2 reduction is catalyzed by Brønsted acid sites. Our mechanism differs from that of Misono in that he proposes that, besides contributing to NO oxidation, a metal site is necessary for hydrocarbon activation [20]. High activity for the NO_2-CH_4 reaction with metal-free catalysts, as seen in Fig. 2and elsewhere [15] confirm that in fact a metal site is not needed for methane activation. In our model, the hydrocarbon reductant is not activated prior to chemisorption. Metal ions and oxides also lead to non-selective reduction of NO_2, i.e., back to NO, which contributes to the lower selectivity of the metal containing catalysts (the other factor being high CH_4 oxidation rates over Na-MOR).

In this study, we provide evidence that the selective reduction of NO_x by hydrocarbons is bifunctional. Furthermore, we observe that either reaction may be rate limiting. At high space velocity or over catalysts with low metal loading, NO oxidation is rate limiting. The rate of N_2 formation increases with metal loading (or presence of metal oxide) and masks the effect of proton sites. Under conditions where NO oxidation is near equilibrium, i.e., catalysts with higher metal loadings and lower space velocities, NO_2 reduction is rate limiting and the rate of N_2 formation increases with increasing number of protons. For the latter reaction conditions, increasing metal loadings have a minimal effect on the rate of reaction.

Based on these concepts, we note that typical catalysts and reaction conditions for lean NO_x reduction are seldom optimized. Increasing the NO oxidation rate by exchange to high metal loadings results in the loss of crucial proton sites. Similarly, catalysts which have many Brønsted sites have low metal loadings and, thus, inadequate NO oxidation activity. For these catalysts, the maximum activity for the overall reaction should be equivalent to that for H-MOR determined for the $NO_2 + CH_4$ reaction. From Fig. 5(a), one would expect that increasing the NO oxidation rate of the H-MOR catalysts might increase the rate of the overall reaction by two to three times.

An initial attempt at such an optimization was performed with a physical mixture of one part CoO_x/NaMOR well mixed with three parts 3% Co/HMOR. Co oxide has a much higher NO oxidation rate than ion exchanged Co and 3% Co/HMOR has nearly as many acid sites as H-MOR. The additional Co in H-MOR may help increase the NO oxidation activity which at 400°C is slow. The results are given in Table 3. If the reaction was simply the mass aver-

Table 3
Overall reaction rate for a physical mixture

Catalyst	Rate of N_2 formation[a] (mol N_2/gm min)	Selectivity
3% Co/H-MOR (3 Co/H)	8.8×10^{-7}	1.09
4% Co/Na-MOR (4 Co/Na)	4.5×10^{-7}	0.26
25% 3 Co/H + 75% 4 Co/Na	12×10^{-7}	0.44
Mass fraction weighted sum of rates	5.6×10^{7}	0.47

[a] 1200 ppm NO, 1000 ppm CH_4, 2.5 wt% O_2, 400°C.

aged rate of the two catalysts, the rate of the mixture would be 5.6×10^{-7} (mol/g min). The experimental rate, 1.2×10^{-6} (mol/g min), was twice as high as the sum of the rates consistent with the bifunctional reaction pathway. Similar results with catalyst mixtures have been recently reported by Resasco [10] and Kung [16]. The selectivity for the physical mixture, at 0.44, was still relatively low compared to the selectivity with HMOR with $NO_2 + CH_4$.

While optimization of catalyst composition may increase the activity, an alternative strategy would be to separate the two functions and simultaneously optimize the catalyst compositions and reaction conditions. The first reaction zone would contain a catalyst with high NO oxidation activity, but low methane oxidation activity. Ideally, the reaction temperature would be low enough such that conversion to NO_2 would be complete. In the second reaction zone, the catalyst would have a high concentration of strongly acidic proton sites. H-ZSM-5 would not be preferred since it has a high NO oxidation/NO_2 decomposition activity. Finally, both catalysts must be stable to SO_x and H_2O under the reaction conditions. This bifunctional catalyst/process optimization will be the focus of future studies.

4. Conclusions

Insight into the reduction of NO_x with methane in excess oxygen has been gained by breaking the overall ($NO + O_2 + CH_4$) reaction into its components, and by isolating the metal and proton functions in Co-mordenite catalysts. The results support a bifunctional mechanism in which the Co sites are responsible for NO oxidation, and the proton sites catalyze the reduction of NO_2 with methane. At 400°C with low metal loadings or high space velocities, NO oxidation is slow and rate limiting. At these conditions the overall rate of reaction is proportional to the Co loading, and the role of proton sites is masked. At high metal loadings or low space velocities, NO oxidation is rapid and NO_2 reduction is rate determining. At this condition, activity is linearly dependent on the number of proton sites. The shift in kinetic regime as a function of metal loading and space velocity rectifies many contradictory conclusions seen in the literature. Finally, more active and selective catalysts can be prepared by independently optimizing the functions of the metal and proton sites.

References

[1] J.N. Armor, Catal. Today 26 (1995) 147.
[2] A.W. Aylor, L.J. Lobree, J.A. Reimer, A.T. Bell, in: Proc. 11th Intl. Congr. Catal. (1996), A-661.
[3] Y. Li, J.N. Armor, J. Catal. 145 (1994) 1.
[4] A.T. Bell et al., paper 60c, 1998, Fall AIChE meeting, Miami (paper in this issue of Catal. Today).
[5] D.B. Lukyanov, G. Sill, J.L. Ditri, W.K. Hall, J. Catal. 153 (1995) 265.
[6] D.B. Lukyanov, G. Sill, J.L. Ditri, W.K. Hall, J. Catal. 163 (1996) 447.
[7] H. Hamada, H. Kintaichi, M. Sasaki, T. Ito, M. Tabata, Appl. Catal. 64 (1990) L1.
[8] K. Yogo, H. Wattan abe Umeneo, E. Kikuchi, Catal. Lett. 19 (1993) 131.
[9] A. Satsuma, K. Yamada, T. Mori, M. Niwa, T. Hattori, Y. Murakami, Catal. Lett. 31 (1995) 367.
[10] C.J. Loughran, D.E. Resasco, Appl. Catal. B: Environ. 7 (1995) 113.
[11] M. Shelef, Chem. Rev. 95 (1995) 209.
[12] E. Kikuchi, K. Yogo, Catal. Today 22 (1994) 73.
[13] E. Kikuchi, M. Ogura, I. Terasaki, Y. Goto, J. Catal. 161 (1996) 465.
[14] M. Misono, Cattech, June 1998, 53.
[15] J.T. Miller, E. Glusker, R. Peddi, T. Zheng, J.R. Regalbuto, Catal. Lett. 51 (1998) 15.
[16] J.-Y. Yan, H.H. Kung, W.M.H. Sachter, M.C. Kung, J. Catal. 175 (1998) 294.
[17] H.S. Fogler, Elements of Chemical Reaction Engineering, third ed., Prentice Hall, 1999.
[18] A. Ribotta, M. Lezcano, M. Kurgansky, E. Miro, E. Lombardo, J. Petunchi, C. Moreaut, J.M. Dereppe, Catal. Lett. 49 (1997) 77.
[19] R.J. Meyer, E. Pietsch (Eds.), Gmelin Handbuch der Anorganischen Chemie, vol. 4, Stickstoff (Verlag Chemie, Berlin, 1936).
[20] S. Yokohama, G. Koyano, M. Misono, paper 63c, 1998 Fall AIChE meeting, Miami (paper in this issue of Catal. Today)
[21] Y. Li, J.N. Armor, J. Catal. 150 (1994) 376.
[22] Y. Li, J.N. Armor, Appl. Catal. B: Env. 2 (1993) 239.
[23] I. Halasz, A. Brenner, K.Y.S. Ng, Catal. Lett. 34 (1995) 151.
[24] A.Y. Stakheev, G.A. Sill, J.L. Ditri, W.K. Hall, Catal. Lett. 38 (1996) 271.
[25] Erratum, J. Catal. 163 (1996) 507.
[26] F. Witzel, G.A. Sill, W.K. Hall, J. Catal. 149 (1994) 229.
[27] E.A. Lombardo, C.W. Lee, S.J. Park, P.J. Chong, J. Catal. 173 (1998) 440.